arTs Università degli Studi di Trieste
Archivio della ricerca – postprint

Probing Peripheral H-Bonding Functionalities in BN-Doped Polycyclic Aromatic Hydrocarbons

Jonathan Tasseroul,[+] Maria Mercedes Lorenzo-Garcia,[+] Jacopo Dosso,[+] François Simon, Simone Velari, Alessandro De Vita, Paolo Tecilla, and Davide Bonifazi*

ABSTRACT: The replacement of carbon atoms at the zigzag periphery of a benzo[*fg*]tetracenyl derivative with an NBN atomic triad allows the formation of heteroatom-doped polycyclic aromatic hydrocarbon (PAH) isosteres, which expose BN mimics of the amidic N*H* functions. Their ability to form H-bonded complexes has never been touched so far. Herein, we report the first solution recognition studies of peripherally NBN-doped PAHs to form H-bonded DD·AA- and ADDA·DAAD-type complexes with suitable complementary H-bonding acceptor partners. The first determination of K_a in solution showed that the 1:1 association strength is around 27 ± 1 M^{-1} for the DD·AA complexes in C_6D_6, whereas it rises to 1820 ± 130 M^{-1} for the ADDA·DAAD array in $CDCl_3$. Given the interest of BN-doped polyaromatic hydrocarbons in supramolecular and materials chemistry, it is expected that these findings will open new possibilities to design novel materials, where the H-bonding properties of peripheral N*H* hydrogens could serve as anchors to tailor the organizational properties of PAHs.

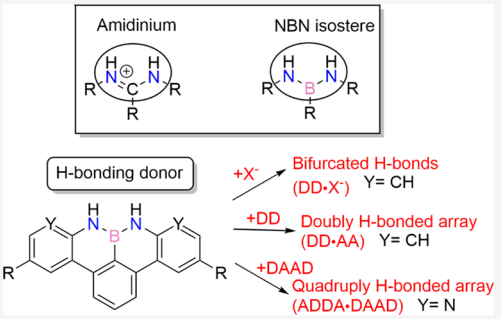

INTRODUCTION

Following the vigorous synthetic developments of polycyclic aromatic hydrocarbons (PAHs),[1] the substitution (i.e., doping) of sp^2-carbon atoms with isoelectronic and isostructural BN couples is re-emerging as a versatile approach to tune the optoelectronic properties of these materials.[2−7] In particular, borazines[8,9] and BN-doped PAHs (e.g., azaborines,[10,11] borazapyrenes,[12,13] borazaphenanthrenes[12,14] borazanaphthalenes,[15,16] borazaanthracene,[17,18] and boraazaperylene[19]) are now increasingly attracting the attention of the physical and chemical community for their use in a broad spectrum of optoelectronic applications.[20−22] When used to decorate a periphery, nonsubstituted BN couples terminate with N*H* functions that, being more acidic than the CH analogues, could engage into H-bonding interactions, as observed with boronic acids.[23] For instance, Liu and co-workers showed in a seminal report that 1,2-dihydro-1,2-azaborine can act as a H-bonding donor in the solid state and engage into a H-bond with the C═O group of a glutamine side chain in a T4 lysozyme.[24,25] However, to the best of our knowledge, no examples of studies describing and measuring the strength of H-bonding interactions in solution with BN-doped peripheries have been reported to date.

While attempting different synthetic strategies to prepare hexabenzo-borazinocoronene,[26] we prepared the NBN-doped isostere of a benzo[*fg*]tetracenyl anion (Figure 1). Derivatives of the NBN-doped isostere were first prepared independently by Hatekeyama et al.[27] and Feng et al.[28] When looking at the NBN-doped zigzag periphery, one can notice that the unsubstituted HNBNH array is a neutral H-bonding mimic of an amidinium moiety, known to establish doubly H-bonded

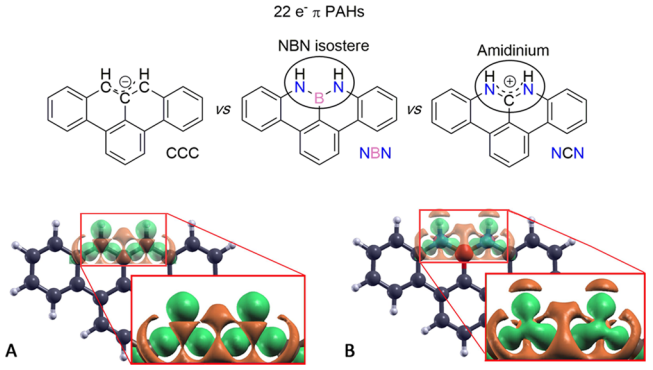

Figure 1. Neutral NBN isosteres of polycyclic aromatic benzo[*fg*]-tetracenyl anions. Charge density distribution for the (A) CCC and (B) NBN-doped scaffold as calculated at the DFT level using the ab initio pseudopotential plane-wave method as implemented in the PWSCF code of the Quantum ESPRESSO distribution (electron density accumulation is depicted in green and depletion in orange).

DD·AA-type arrays. Density functional theory (DFT) calculations (see the Supporting Information for details) on the all-carbon analogue (CCC) and its NBN-doped isostere suggest that the highest occupied molecular orbital (HOMO) and lowest unoccupied molecular orbital (LUMO) distributions are very similar on both molecules, with the NBN atomic triad negligibly contributing to the LUMO (Figure S39) in line with the data reported by Hatekeyama et al.[27] and Feng et al.[28] Remarkably, the lack of contribution from the B atom is observable for the LUMO orbital, advocating a tenuous electrophilic character of the B atom center (Figure S39). On the other hand, a significant contribution from the N atoms is noticeable for the HOMOs with the involvement of the B atom remaining negligible. As expected, the NBN-doping results in a low-lying HOMO, the latter contributing significantly to the increase in the HOMO−LUMO gap with respect to the 22−π−e^- all-carbon benzo[*fg*]tetracenyl derivative (Figure S39).

DFT calculations also reveal a peculiar distribution of the electron density around the N*H* group, as shown by the charge density transfer plots (calculated as $\rho_{mol} - \Sigma\rho_{atom}$, where ρ_{mol} is the charge density of the molecule and ρ_{atom} is the density of the single atoms) in Figure 1b. The decrease in charge density for the aminic H atoms is induced by the presence of the electronegative N atoms and is clearly visible in the NBN-doped molecule, while it is absent for the iso-positional H atoms of the CCC analogue (Figure 1a). As observed by Liu and co-workers,[17] this suggests that the N*H* groups are acidic, thus possibly enabling the formation of double H-bonding interactions in the presence of a suitable H-bond acceptor. Electrostatic potential (ESP) calculations showed that molecule **1** displays great charge depletion on the N*H* groups and B atoms, whereas the carbocyclic backbone remains slightly negatively charged (Figure 2). These results are

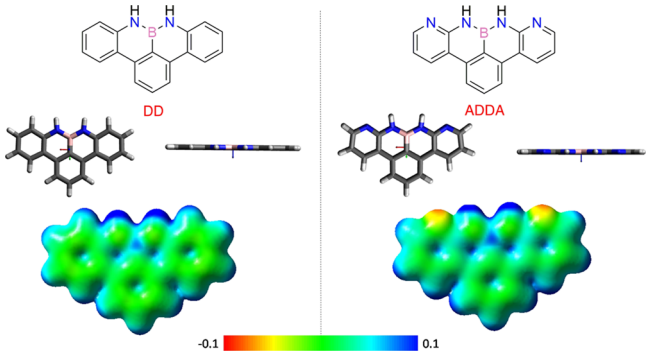

Figure 2. DFT calculations at the B3LYP/6-31+G** level of theory of the structural and ESP properties of the NBN-doped benzo[*fg*]-tetracenyl derivatives exposing H-bonding recognition DD-type (left) and ADDA-type (right) arrays.

consistent with the calculated electron density properties, further suggesting that this peculiar NBN motif can be considered as a neutral isostere of substituted amidinium cations, known to behave as a H-bonding DD-type array.[29] This prompted us to study the H-bonding abilities of the NBN-doped moiety toward suitable complementary H-bonding acceptors, such as fluoride ions and complementary AA-type H-bonding guests. Thus, we synthesized NBN-doped benzo[*fg*]tetracenyl derivatives **1** and **2**, which should undergo formation of bifurcated and doubly H-bonded arrays with F^- ions and 1,8-naphthyridine, respectively (Figure 3). When comparing the H-bonding NBN-doped array with that of the

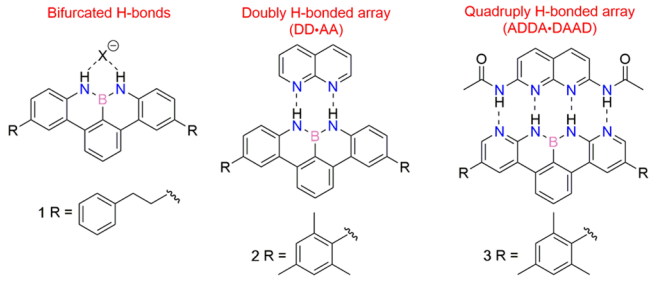

Figure 3. H-bonded arrays and recognition modes studied in this work.

amidinium, one can hardly fail to notice that the amidinium is expected to present the strongest association due to the presence of charge−dipole interactions. Building on this hypothesis, we conjectured that the BN-doped scaffold **3**, in which the lateral fused benzene rings have been substituted by two pyridines, should behave as an ADDA-type H-bonding motif (Figure 3). In the presence of a suitable complementary H-bonding DAAD-type partner, molecule **3** is expected to form quadruply H-bonded ADDA·DAAD arrays featuring higher association constants than those hypothesized for DD·AA complexes. For this reason, we also prepared receptor **3** and studied its H-bonding recognition properties in the presence of diacetyl-2,7-diaminonaphthyridine (Figure 3). All molecules were equipped with either 2-phenylethyl chains (**1**) or mesitylene moieties (**2** and **3**) to increase solubility in organic solvents.

RESULTS AND DISCUSSION

Synthesis and Structural Characterization. We synthesized the NBN core starting from the relevant aniline bearing the chosen solubilizing group instead of performing post-synthetic functionalization of the NBN-doped benzo[*fg*]-tetracenyle. This choice allowed us to obtain differently substituted HNBNH derivatives without the need of protecting groups for the aminic moieties. Moreover, to increase the synthetic versatility of the route, we decided to explore cyclization conditions for the preparation of the NBN-doped PAHs that start from an unsubstituted polyphenylene scaffold. The syntheses of the three aniline precursors are reported in the insets of Scheme 1. The first step of the synthesis of **6** is the Pd/Cu-catalyzed Sonogashira cross-coupling of *para*-iodoaniline with phenylacetylene, yielding phenylacetylene-aniline **4**.[30]

Its reduction with Pd/C in MeOH afforded phenethylaniline **5**, which was transformed into 3-bromoaniline **6** in an 85% yield by the bromination reaction with *N*-bromosuccinimide (NBS) at room temperature (rt). Similarly, anilines **9** and **11** were obtained starting from the Suzuki−Miyaura cross-coupling reaction between 2,4,6-trimethylphenylboronic acid and either *p*-bromonitrobenzene or 2-amino-5-bromopyridine- to give intermediates **7** and **10** in 58 and 95% yields, respectively. Nitro-derivative **7** was reduced with AcOH/Zn (88% yield), and the resulting amine was brominated with NBS at rt to give substituted aniline **9** in a 75% yield. Analogously, bromination of **10** with NBS gave final aniline **11** in excellent yield (87%). The aniline precursors were then cross-coupled through the Suzuki−Miyaura reaction with

Scheme 1. Synthetic Routes toward Aniline Precursors 6, 9, and 11 (Above) and NBN-Doped Scaffolds 1, 2, and 3 (Below).

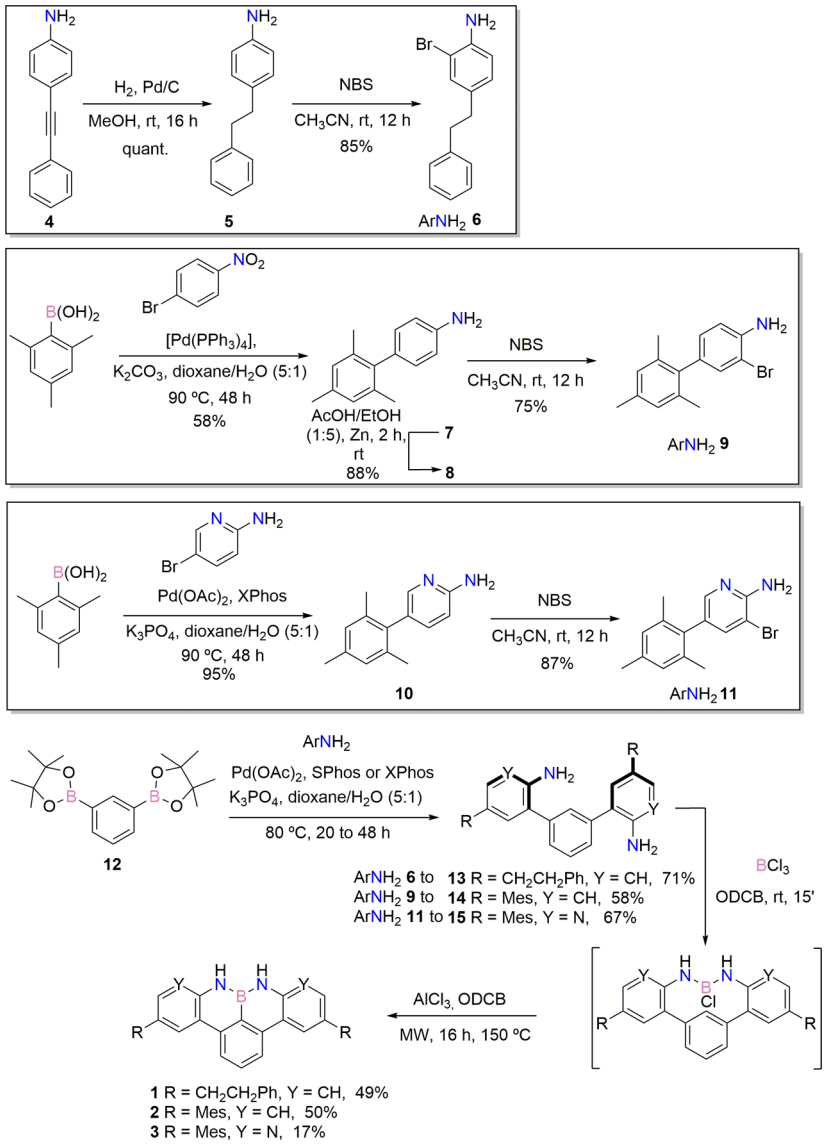

phenylene bisboronate **12** in the presence of $Pd(OAc)_2$, SPhos (or XPhos), and K_3PO_4 to give bis-aniline intermediates **13**, **14**, and **15** in 71, 58, and 67% yields, respectively (Scheme 1). Our synthetic studies to prepare NBN-doped PAH by cyclization on an unsubstituted aromatic scaffold were commenced using bis-aniline **13** as a substrate. Building on a general borylation procedure following modified versions of the approaches previously described by Dewar and later by Hatakeyama et al.,[20] in a first attempt, we performed an intramolecular Friedel−Crafts cyclization reaction starting from the amino-BCl_3 intermediate in the presence of $AlCl_3$ in ODCB at 150 °C. Unfortunately, these conditions were unsuccessful, and no conversion was observed. Similarly, deprotonation of bis-aniline **13** with two equivalents of *n*-BuLi at −84 °C followed by the addition of BCl_3 at rt and Friedel−Crafts cyclization reaction did not lead to any transformation, and only the starting material was recovered. On the other hand, changing the conventional oil-bath heating to microwave irradiation, 100% conversion was observed, affording the desired molecule **1** in 49% yield after purification. As expected, no reaction took place in the absence of $AlCl_3$, even when two equivalents of BCl_3 were used. Subjecting amino-precursors **14** and **15** to the same procedure, compounds **2** and **3** were obtained in 50 and 17% yields, respectively. All three compounds exhibit excellent chemical and thermal stability. The structures of all intermediates and products were unambiguously identified by high-resolution mass spectrometry (HRMS) through the detection of the peak corresponding to the molecular mass of the ion (M^+) and by ^{1}H-nuclear magnetic resonance (^{1}H-NMR), ^{13}C-NMR, ^{11}B-NMR, and infrared (IR) spectroscopies (see Figures S1−S29, Supporting Information). The exemplary ^{1}H-NMR spectra of NBN-doped derivatives **1** in THF-d_8 and **3** in $CDCl_3$ are reported in Figure 4. Proton resonances $H(a)$, $H(b)$, and $H(c)$ of structure **1** appear distinctively as a triplet at 7.67 ppm, a doublet at 8.11 ppm, and a broad singlet at 8.05 ppm, respectively. These three signals are highly deshielded, confirming the polycyclic aromatic character of the structure. The signal of the N*H* protons appears as a broad singlet centered at 7.31 ppm. Similarly, for molecule **3**, the $H(b)$ and $H(a)$ resonances appear at 8.31 and 8.15 ppm, respectively. The $H(g)$− and $H(h)$− peaks are visible as a doublet and

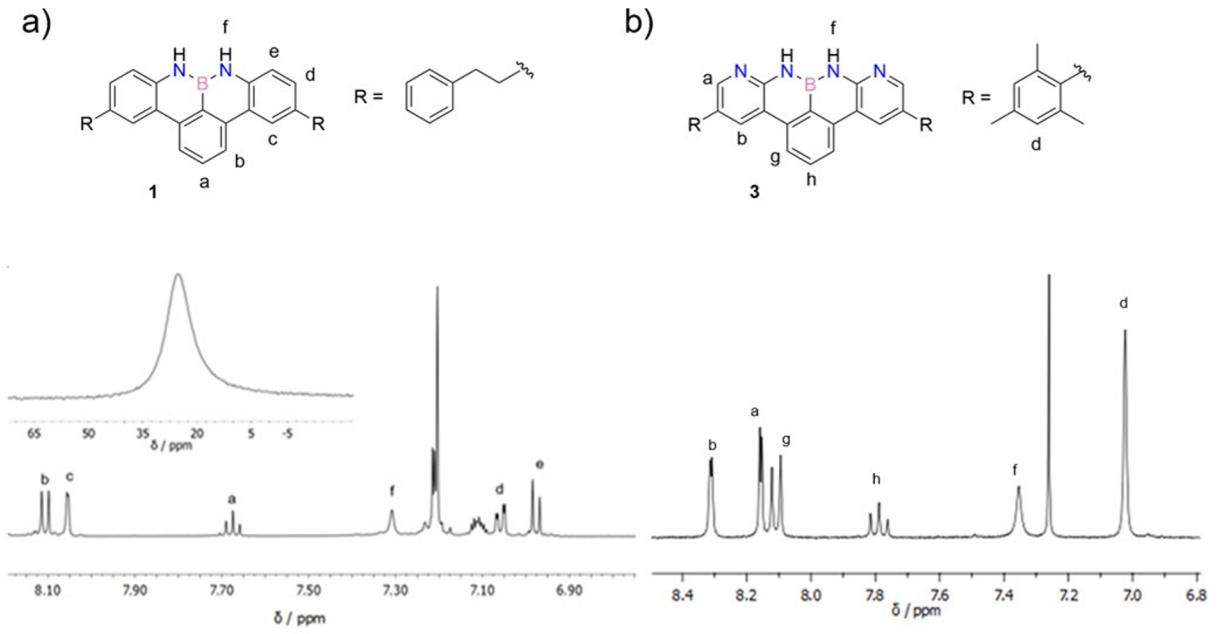

Figure 4. (a) ^{1}H-NMR and ^{11}B-NMR spectra for **1** in THF-d_8 at 298 K and (b) ^{1}H-NMR spectra of **3** in $CDCl_3$ at 298 K.

triplet at 8.11 and 7.79 ppm followed by the resonances of the N*H*(*f*) protons at 7.36 ppm. The ^{11}B-NMR spectrum of **1** (Figure 4, inset) displays a broad peak centered at 26.4 ppm, the chemical shift of which is in agreement with that reported for similar NBN triads.[31,32]

The photophysical properties of molecule **1** were investigated in THF solutions (see Figure S30, Supporting Information). Emission measurements display blue fluorescence with a Φ_{fl} value of 21% (reference anthracene, λ_{exc} = 372 nm), with the spectrum displaying a mirror image of the two lowest-energy absorption bands. The Stokes shift was as small as 27 nm, indicating good rigidity of the structure, as expected for a fully fused PAH. The optical gap (E_{00}) of **1**, deduced from the highest emission energy peak, has been calculated to be 3.22 eV. Cyclic voltammetry (Figure S33) of **1** in THF shows a clear reversible mono-electronic oxidative wave at 0.4 V (vs Fc/Fc^{+}). This allowed us to calculate the HOMO and LUMO energy levels, which revealed to be −5.51 and −2.29 eV, respectively (the LUMO energy level was estimated from E_{00}). Overall, these data are in agreement with those reported for the unsubstituted NBN derivative in CH_2Cl_2 and predicted by DFT calculations (Figure S39).[27,28]

Titration Experiments and Determination of the H-Bonding Recognition Abilities. We started with the F^- ions as probes to study the recognition properties of molecule **1** toward bifurcated H-bonded complexes. The interaction was studied in THF solution through spectroscopic UV-vis absorption titration experiments (Figure 5). In particular, a standard solution of TBAF was added stepwise to a 4.43 × 10^{-5} M solution of **1** at 298 K and the steady-state UV-vis absorption spectra taken (Figure 5). Upon addition of increasing concentration of TBAF, the intensity of the band centered at 360 nm decreases, and a new transition develops at 390 nm. A similar red shift of the lowest-energy band had been previously observed when fluoride ions interact with other DD-type H-bonding systems, such as urea derivatives.[33,34] Notably, no marked color changes were observed during the titration experiments, suggesting that molecule **1** likely does

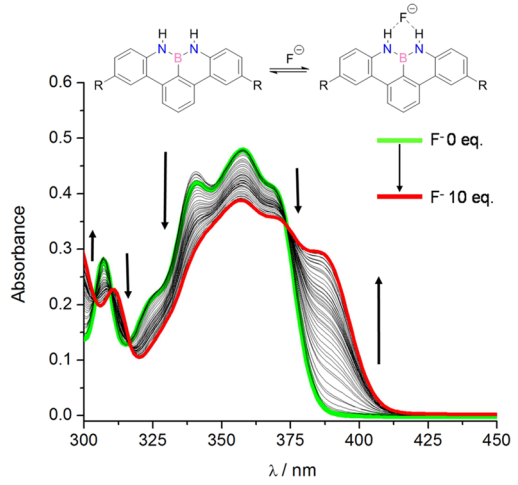

Figure 5. UV-vis titrations of **1** (c_0 = 4.43 × 10^{-5} M) in THF at 298 K with TBAF.

not undergo deprotonation (see also Figures S31 and S32 for the color change and UV-vis spectra of the mono- and bis-anionic species obtained upon addition of one and two equivalents of *sec*-BuLi). Complementary ^{1}H-NMR titrations with a 1 × 10^{-3} M solution of **1** (Figure S38) showed a fast equilibrium, triggering a progressive downfield shift of the N*H* protons from 7.30 to 10.60 ppm upon the incremental addition of TBAF. Together with the *H*(*f*) resonances, also the signals of the aromatic peri-protons *H*(*e*) experience a progressive deshielding upon stepwise addition of TBAF, confirming the frontal arrangement of the H-bonded complex. However, the signal of the N*H* protons in the presence of up to 2 equiv of TBAF is rather broad, almost not detectable, and, in the presence of larger excess of fluoride, remains broad and nonsymmetric. This hampered a quantitative determination of the association constant (K_a) in THF. Moreover, it is likely that the equilibrium is made more complex by concurrent additional equilibria, such as the formation of the correspond-

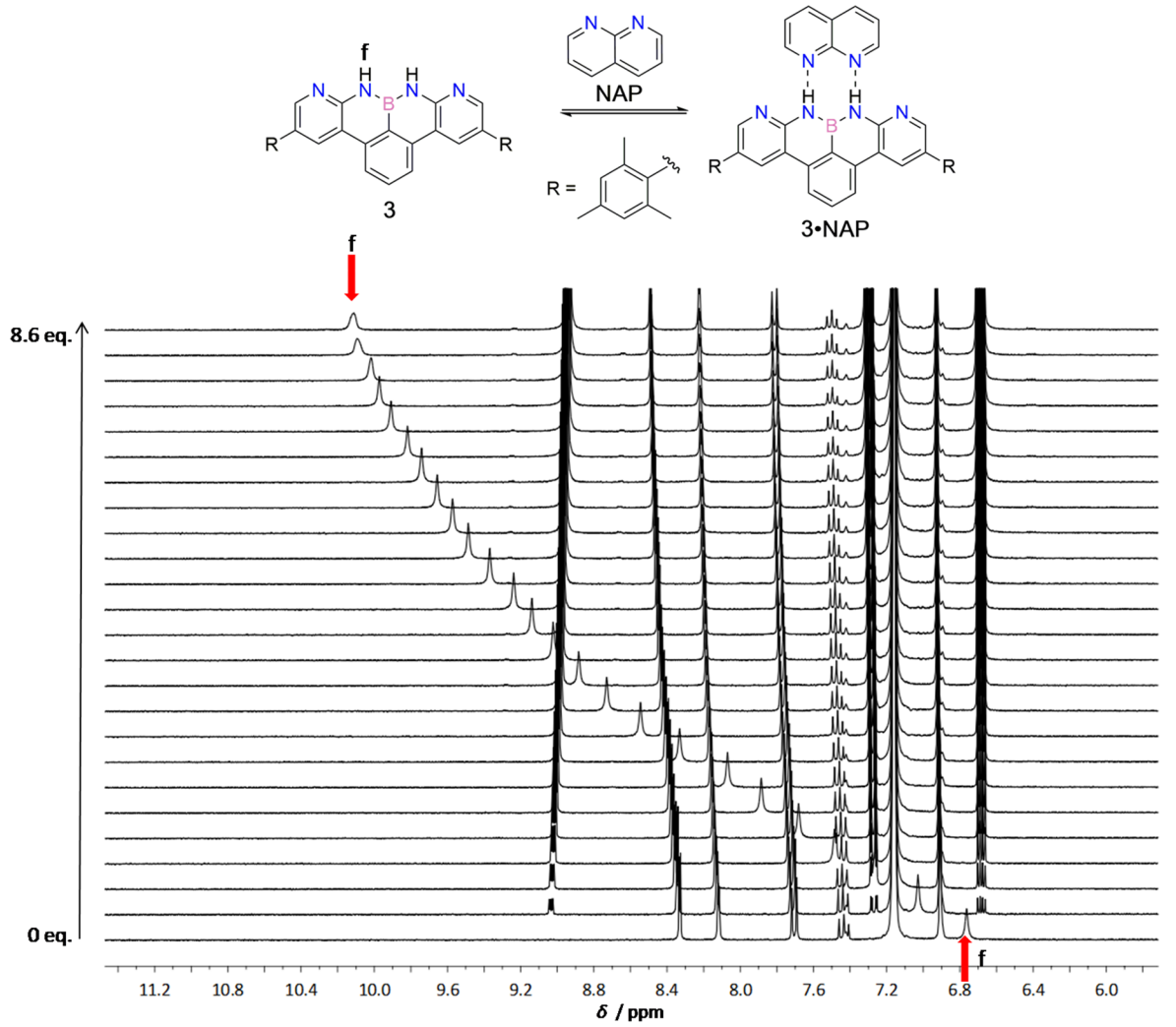

Figure 6. ^{1}H-NMR (400 MHz) titration of **3** (c_0 = 9.30 × 10^{-3} M) with **NAP** in C_6D_6 at 298 K.

ing bihalide species (HF_2^-), which is known to take place in organic solvents.[35]

Complementary ^{11}B-NMR studies showed that the chemical shift of the B resonance is unaffected by the incremental addition of TBAF (Figure S38), thus excluding the presence of any competitive interactions established between the B center and the F^- ions, further confirming the formation of H-bonded complex **1**·F^- in solution. This is in line with the theoretical findings, which revealed an elusive contribution of the B atom to the LUMO orbital of **1**.

To further investigate H-bonding properties of the NBN-doped PAHs, we studied the binding of molecules **2** and **3** with 1,8-naphthyridine (**NAP**) and diacetyl-2,7-diaminonaphthyridine (**DAN**).[36] While **NAP** should form doubly H-bonded DD·AA arrays with **2** and **3**, **DAN** should provide quadruply ADDA·DAAD complexes with **3** (Figure 3). Addition of increasing amount of **NAP** to an 8 mM solution of **3** in CD_2Cl_2 up to 2.5 equiv led to a minor linear downfield shift of the *H*(*f*) resonances, suggesting the formation of a H-bonded complex with a low K_a value (Figure S34). This was confirmed by changing the solvent to less polar and less competitive C_6D_6, in which the formation of H-bonds is favored (Figure 6).[37]

Upon addition of increasing amount of **NAP** (up to 8.6 equiv) to a 9.30 × 10^{-3} M solution of **3** in C_6D_6, a large downfield shift (>3.3 ppm) of the *H*(*f*) protons was observed, typical of the formation of a H-bonded complex under a regime of fast equilibrium exchange (Figure 6). Together with the *H*(*f*) resonances, also the peaks of the proton resonances of the lateral pyridyl moieties revealed significant downfield shifts upon addition of **NAP**, confirming the frontal arrangement of the H-bonded DD·AA complex. The same picture is obtained by titrating molecule **2** with **NAP** in C_6D_6 (see Figure S36). Fitting the chemical shift values of the *H*(*f*) resonances from the titration experiments of **3** and **2** with **NAP** to a 1:1 binding isotherm with Dynafit[38] gave K_a values of 25 ± 1 and 27 ± 1 M^{-1} for complexes **3**·**NAP** and **2**·**NAP**, respectively (Figures S35 and S36). Notably, these H-bonded DD·AA-type complexes show association strengths considerably lower than those observed with a series of aromatic boronic acids that, in their *syn*−*syn* conformation, showed 1:1 association in the range between 300 and 6900 M^{-1}.[23] Further evidence of the ability of the NBN motif to undergo H-bonding recognition and form supramolecular complexes came from the titration studies of molecule **3** with complementary DAAD-type **DAN** derivative. As **DAN** is almost insoluble in benzene, the titration was performed in the more polar and more competitive $CDCl_3$ solvent. As shown in Figure 7, titration of a 4.94 × 10^{-3} M solution of **3** with increasing amounts of **DAN**, up to 3.36 equiv resulted in a large downfield shift (>3.3 ppm) of the

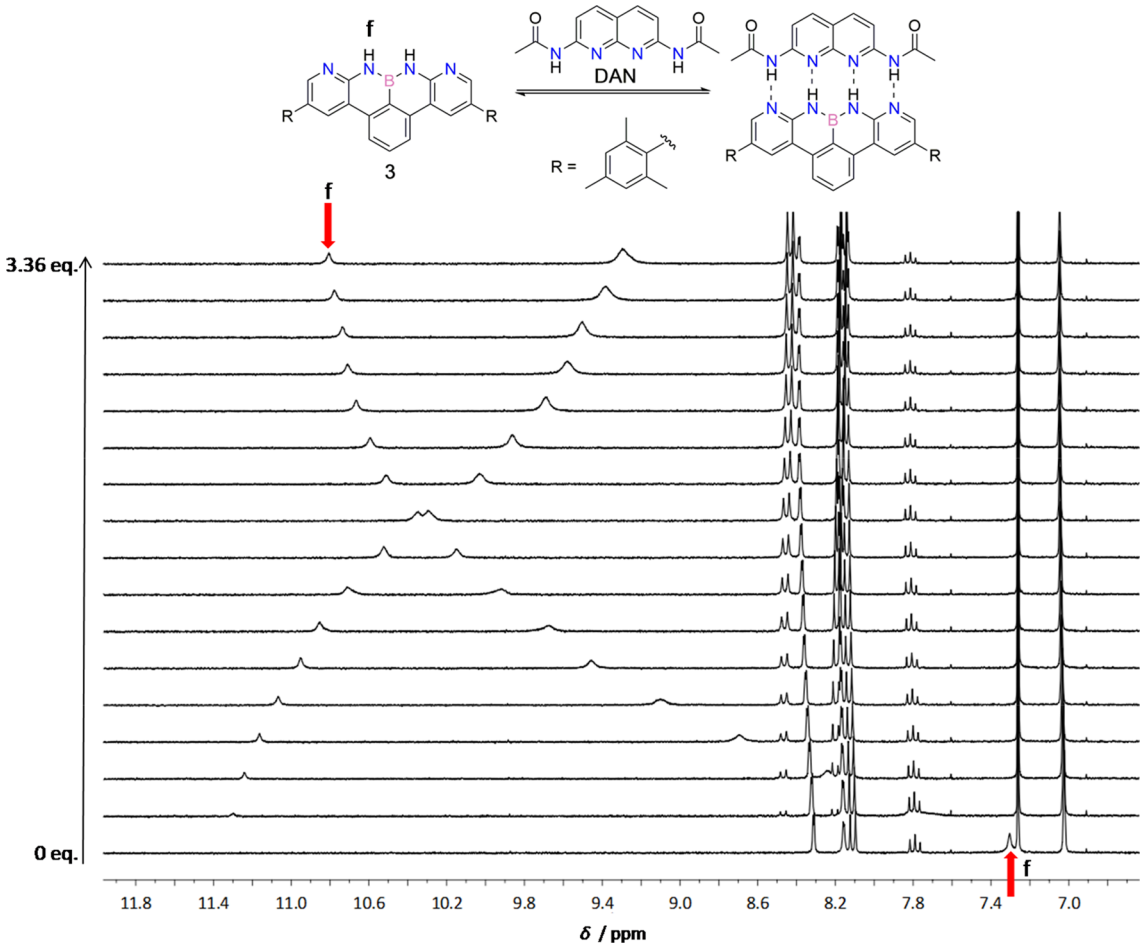

Figure 7. ^{1}H-NMR (300 MHz) titration of receptor **3** (c_0 = 4.94 × 10^{-3} M) with **DAN** in $CDCl_3$ at 298 K.

H(*f*) resonances. This suggested the formation of a frontal H-bonded ADDA·DAAD complex. The calculated K_a value for the 1:1 complex **3·DAN** was found to be 1820 ± 130 M^{-1} in $CDCl_3$, which is more than 70 times higher than that measured for the **3·NAP** in C_6D_6. Job's analysis of the titration data confirmed the 1:1 stoichiometry of the quadruply H-bonded **3·DAN** complex (Figure S37).

Despite the numerous attempts, we could not grow suitable crystals for X-ray diffraction analysis of both the single components (**1**, **2**, and **3**) and H-bonded complexes (**2·NAP**, **3·NAP**, and **3·DAN**). Therefore, we turned our attention to NOESY experiments to confirm the structure of the hypothesized hydrogen-bonded complex. The ^{1}H−^{1}H NOESY spectrum of a 7.0 × 10^{-3} M solution of **3** in the presence of 1.1 equiv of **DAN** was recorded (Figure 8). From this analysis, one can easily discern a through-space interaction (Figure 8a) between protons *H*(*b*) and *H*(*g*), which allowed the unambiguous assignment of the resonances attributed to *H*(*a*) and *H*(*b*). A clear peak assignment could not be made from the ^{1}H−^{1}H COSY spectra (Figure S16). Interestingly, the through-space interaction between protons *H*(*i*) of the Me groups of **DAN** and protons *H*(*a*) of **3** (Figure 8b) suggests that close spatial proximity exists for these atoms, unambiguously confirming the structure of the proposed frontal H-bonding arrangement for complex **3·DAN**.

CONCLUSIONS

In conclusion, in this paper, we describe the synthesis of a family of NBN isosteres of a full-carbon benzo[*fg*]tetracenyl anion with improved solubility in different organic solvents. The NBN functional group could be inserted in a zigzag topology, allowing the planarization of the three aryl rings. DFT calculations of the charge density showed significant charge depletion at the N*H* protons, anticipating good H-bonding capabilities of this NBN functional group. This was for the first time demonstrated by spectroscopic titration of molecule **1** with F^- ions, which clearly showed the formation of H-bonded complex **1·F**$^-$ excluding any interactions with the B center. Titration of molecules **2** and **3** with complementary H-bonding **NAP** and **DAN** showed that heteromolecular H-bonded complexes **2·NAP**, **3·NAP**, and **3·DAN** could be formed. In particular, the complex **3·DAN** presents a quadruply H-bonded array with a K_a value of 1820 ± 130 M^{-1} in $CDCl_3$. These findings open new applicative horizons for the BN doping of polyaromatic hydrocarbons in supramolecular chemistry, for which the ability to form H-bonding interactions at the periphery can be exploited both in solution and at the solid state.[40] In addition, the ease of preparing these BN-doped PAHs makes these heterocycles interesting to organic, supramolecular, and materials chemists who are incessantly looking for programmable synthetic strategies for digitizing molecules displaying multifunctional and self-organization properties exploitable in materials science and biology.[41]

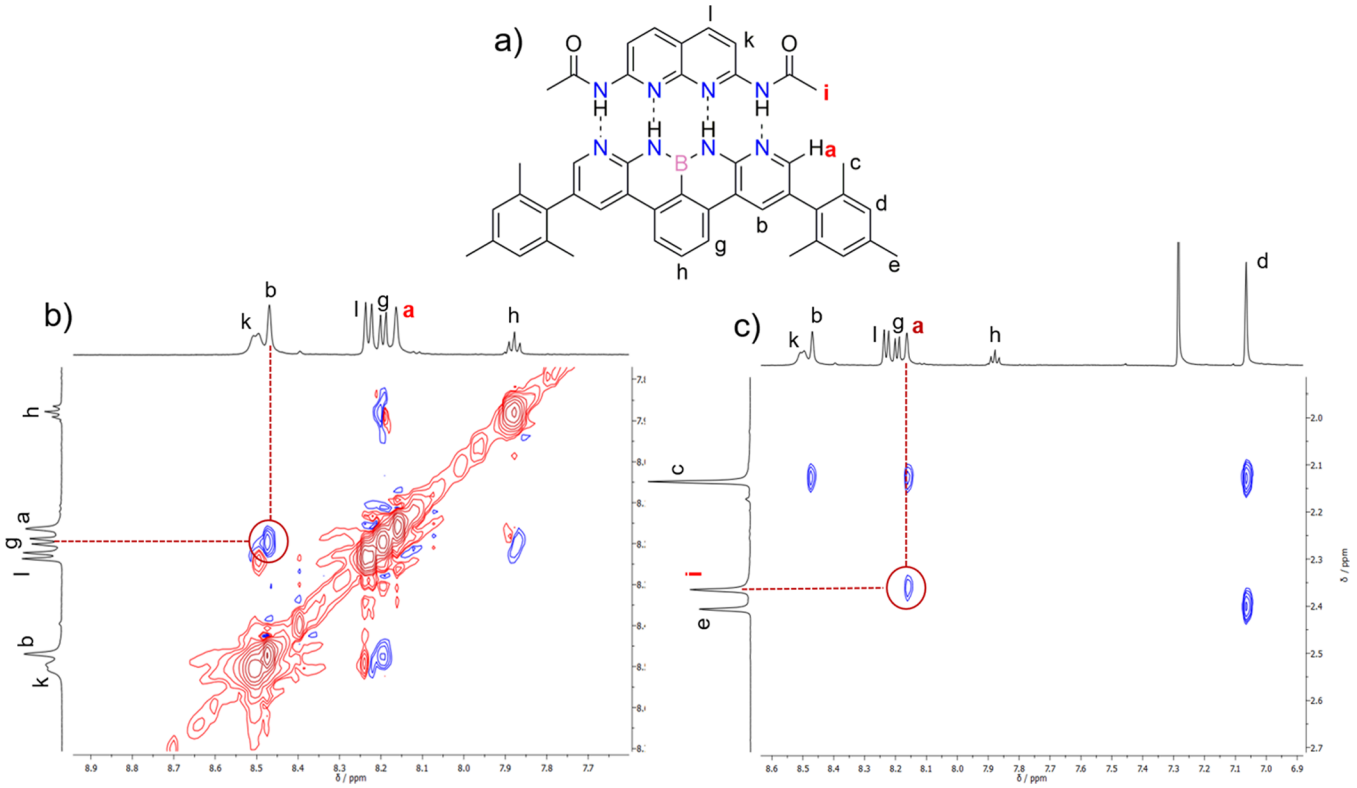

Figure 8. (a) Arrangement of hydrogen-bonded aggregates; 2D ^{1}H-NOESY NMR (600 MHz) of receptor **3** (c_0 = 7.0 × 10^{-3} M) with **DAN** in $CDCl_3$ at 298 K; ratio of **3** to **DAN**: 1:1.1. (b) Detail of aromatic part with through-space interaction between $H(b)$ and $H(g)$ highlighted. (c) Zoom on the through-space interaction between $H(a)$ and $H(i)$.

EXPERIMENTAL PART

Instrumentation, Materials, and General Methods. Thin-layer chromatography (TLC) was performed on a Macherey-Nagel Alugram SIL G/UV_{234} 0.20 mm and visualized by UV light (254 or 366 nm). Microwave irradiation (MW Irr.) was performed with a Biotage AB Initiator 2.5 in 2, 5, and 20 mL sealed tubes, producing controlled irradiation at 2.450 GHz. The reaction temperature was monitored with an external surface sensor. Adsorption silica column chromatography (SCC) was performed on Merck Gerduran silica gel 60 (40−63 μm), used with a Büchi Sepacore X50 flash system. Melting points (M.P.) were recorded on a Büchi Melting Point B-545 in open capillaries without correction. Nuclear magnetic resonance analysis (^{1}H-NMR, ^{13}C-NMR, and ^{11}B-NMR) spectra were recorded on Jeol JNM EX-400, Jeol JNM ECZR-500, and Bruker Fourier 300 MHz spectrometers equipped with a dual (^{13}C-NMR and ^{1}H-NMR) probe, a Bruker AVANCE III HD 400 MHz NMR spectrometer equipped with a broadband multinuclear (BBFO) SmartProbe, a Bruker AVANCE III HD 500 MHz spectrometer, or a Bruker 600 MHz Advance 3 equipped with broadband multinuclear (BBO) Prodigy CryoProbe. For ^{1}H and ^{13}C, chemical shifts are reported in ppm downfield from tetramethylsilane using the residual solvent signals as an internal reference ($CDCl_3$ δ_H = 7.26 ppm, δ_C = 77.16 ppm; CD_2Cl_2 δ_H = 5.32 ppm, and δ_C = 53.84 ppm). For ^{11}B, chemical shifts are reported in ppm downfield from $BF_3{\cdot}OEt_2$ as an internal reference, and analyses were performed in quartz tubes. Coupling constants (J) are given in Hz. The resonance multiplicity is described as s (singlet), d (doublet), t (triplet), q (quartet), dd (doublet of doublet), m (multiplet), and br s (broadened signal). All spectra were recorded at 25 °C, unless otherwise specified. For ultraviolet−visible absorption spectroscopy (UV−Vis) and emission, the UV−Vis absorption spectra were recorded on an Agilent Cary 5000 UV−Vis−NIR spectrophotometer. All absorption measurements were performed at 25 °C, unless otherwise specified. The estimated experimental errors are 2 nm on the band maximum, 5% on the molar absorption coefficient, and 10% on the emission quantum yield in solution. The emission spectra were recorded on an Agilent Cary Eclipse fluorescence spectrofluorimeter. All fluorimetric measurements were performed at 25 °C, unless otherwise specified. Quantum yield values in solution are calculated using anthracene in air-equilibrated ethanol (Φ = 0.27),[42] following the method of Demas and Crosby.[43] For infrared (IR) absorption spectroscopy, the spectra were recorded on (i) a Perkin-Elmer Spectrum II FT-IR System UATR mounted with a diamond crystal (selected absorption bands are reported by wavenumber (cm^{-1})) and (ii) a Shimadzu IR Affinity 1S FTIR spectrometer in ATR mode with a diamond mono-crystal. Matrix-assisted laser desorption−ionization time-of-flight mass spectrometry analysis (MALDI-TOF) was performed by the Centre de Spectrométrie de Masse at the Université de Mons in Belgium using the following instrumentation: a Waters QToF Premier mass spectrometer equipped with a nitrogen laser, operating at 337 nm with a maximum output of 500 mW delivered to the sample in 4 ns pulses at 20 Hz repeating rate. Time-of-flight analyses were performed in the reflectron mode at a resolution of about 10,000. The matrix solution (1 μL) was applied to a stainless-steel target and air-dried. Analyte samples were dissolved in a suitable solvent to obtain 1 mg/mL solutions. One microliter aliquots of these solutions were applied onto the target area already bearing the matrix crystals and air-dried. For the recording of the single-stage MS spectra, the quadrupole (rf-only mode) was set to pass ions from 100 to 1000 THz, and all ions were transmitted into the pusher region of the time-of-flight analyzer where they were analyzed with 1 s integration time. Electrospray ionization time-of-flight mass spectrometry analysis (ESI-TOF) was performed at Cardiff University using a Waters LCT HR TOF mass spectrometer in the positive or negative ion mode for high-resolution ESI mass spectra.

Calculations. DFT calculations were performed using the ab initio pseudopotential plane-wave method as implemented in the PWSCF code of the Quantum ESPRESSO distribution,[44] using Ultrasoft pseudopotentials from the publicly available repository.[45] For the exchange-correlation term, a GGA-BLYP approximation has been

used.[46,47] The valence electronic wave functions were expanded onto a plane-wave basis set with a kinetic energy cutoff of 544 eV. The Brillouin zone integration for the gas-phase systems investigated has been limited to the Γ-point only. Ball-and-stick models are rendered using XCrySDen software.[48]

Reagents and Solvents. Reagents were purchased from Sigma-Aldrich, Acros Organics, Fisher Scientific, Tokyo Chemical Industry (TCI Europe), ABCR, Carbosynth, and/or Apollo Scientific and used as received, unless noted otherwise. **NAP** (1,8 naphthyridine) was acquired from Fluorochem or TCI and used as received. Solvents were purchased from Sigma-Aldrich, while deuterated solvents from Eurisotop. Anhydrous conditions were obtained by heating glassware in an oven at 120 °C for 4 h or by three cycles of heating with a heat gun under argon or nitrogen flow and cooling down under vacuum. The inert atmosphere was maintained using argon- or nitrogen-filled balloons connected to a syringe and needle penetrating rubber stoppers used to close the flasks' necks. Solutions were degassed using the freeze-pump-thaw technique: solutions were frozen using liquid nitrogen and kept under vacuum for 10 min before thawing. ODCB (*o*-dichlorobenzene) was distilled from CaH_2 with reduced pressure and stored over 5 Å molecular sieves. All reactions were performed under anhydrous and inert gas conditions, unless otherwise specified. Reactions were heated using silicon oil baths, and the temperature was monitored with an external probe, unless otherwise specified.

Experimental Procedures. *4-(Phenylethynyl)aniline (**4**).* Diisopropylamine (80 mL) was degassed with four freeze-pump-thaw cycles in a flame-dried Schlenk. 4-Iodoaniline (3.5 g, 16 mmol), $[Pd(PPh_3)_2Cl_2]$ (112 mg, 0.16 mmol), CuI (61 mg, 0.32 mmol), and phenylacetylene (2.11 mL, 19.2 mmol) were added, and the suspension was stirred overnight at rt under argon. The black suspension was diluted with EtOAc (100 mL), washed with H_2O (100 mL × 3) and brine (100 mL). The organic phase was dried on Na_2SO_4 and evaporated to a dark brown solid; purification by SCC (Cy/EtOAc 0 to 20%) afforded compound **4** as a white solid[30] (3.5 g, 99%). M.P.: 119−121 °C. ^{1}H-NMR (400 MHz, $CDCl_3$): δ 3.82 (br s, 2H), 6.64 (d, 2H, J = 8.8 Hz), 7.29−7.35 (m, 5H), 7.50 (dd, 2H, J = 8.0 Hz, J_2 = 1.4 Hz). ^{13}C{^{1}H}-NMR (100 MHz, $CDCl_3$): δ 87.4, 90.3, 112.4, 114.8, 123.9, 127.7, 128.4, 131.4, 133.0, 146.8. IR: 472, 498, 518, 535, 690, 756, 826, 846, 914, 966, 1068, 1137, 1179, 1290, 1317, 1371, 1440, 1486, 1513, 1591, 1615, 2210, 3036, 3377, 3475 cm^{-1}. HRMS (EI-TOF) m/z: $[M]^+$ calcd for $C_{14}H_{11}N^+$, 193.0886; found, 193.0888.

*4-Phenethylaniline (**5**).* 4-(Phenylethynyl)aniline **4** (2.42 g, 12.5 mmol) was dissolved in MeOH (50 mL) under an argon atmosphere, and Pd/C (10%, 267 mg, 0.25 mmol) was added. Argon was replaced with H_2, and the suspension was stirred at rt for 24 h. The reaction mixture was filtered on a celite pad and evaporated to a yellow residue; purification on a silica plug (Cy/EtOAc 30%) afforded molecule **5** as a white solid (2.44 g, quant.). M.P.: 51−53 °C. ^{1}H-NMR (400 MHz, $CDCl_3$): δ 2.65 (m, 4H), 3.48 (br s, 2H), 6.63 (d, 2H, J = 8.4 Hz), 6.98 (d, 2H, J = 8.4 Hz), 7.17−7.30 (m, 5H). ^{13}C{^{1}H}-NMR (100 MHz, $CDCl_3$): δ 37.1, 38.3, 115.2, 125.8, 128.3, 128.5, 129.2, 131.8, 142.1, 144.4. IR: 523, 696, 747, 764, 810, 858, 1027, 1065, 1143, 1175, 1261, 1451, 1491, 1512, 1616, 2849, 2912, 3023, 3348 cm^{-1}. HRMS (AP-TOF) m/z: $[M + H]^+$ calcd for $C_{14}H_{16}N^+$, 198.1283; found, 198.1285.

*2-Bromo-4-phenethylaniline (**6**).* 4-Phenethylaniline **5** (1.7 g, 8.6 mmol) was stirred in CH_3CN (60 mL) with NBS (1.5 g, 8.6 mmol) for 12 h. The solution was diluted with EtOAc (150 mL), washed with $Na_2S_2O_3$ (sat.) (100 mL), H_2O (100 mL × 2), brine (100 mL), dried on $MgSO_4$, and evaporated. The residue was purified by SCC (Pet. Et/EtOAc, 0 to 5%) to afford molecule **6** as a pale brown solid (2.0 g, 85%). M.P.: 47−49 °C. ^{1}H-NMR (400 MHz, CD_2Cl_2): δ 2.79−2.88 (m, 4H), 4.00 (br s, 2H), 6.69 (d, 1H, J = 8.0 Hz), 6.93 (dd, 1H, J = 8.0 Hz, J_2 = 1.4 Hz), 7.18−7.31 (m, 6H). ^{13}C{^{1}H}-NMR (100 MHz, CD_2Cl_2): δ 36.6, 38.0, 108.9, 115.7, 125.9, 128.3, 128.5, 128.6, 132.2, 133.1, 141.8, 142.3. IR: 481, 498, 560, 602, 675, 696, 739, 814, 889, 1033, 1079, 1155, 1202, 1265, 1305, 1411, 1452, 1496, 1600, 1616, 1711, 2856, 2922, 3026, 3336, 3420 cm^{-1}. HRMS (EI-TOF) m/z: $[M]^+$ calcd for $C_{14}H_{14}BrN^+$, 275.0304; found, 275.0307.

*1,3-Bis(4,4,5,5-tetramethyl-1,3,2-dioxaborolan-2-yl)benzene (**12**).* Anhydrous DMF (20 mL) was degassed with five freeze-pump-thaw cycles in a flame-dried Schlenk. B_2pin_2 (6.5 g, 25.4 mmol), $[Pd(dppf)Cl_2]\cdot CH_2Cl_2$ (350 mg, 0.43 mmol), and AcOK (3.3 g, 33.6 mmol) were added, and three freeze-pump-thaw cycles were performed. 1,3-Dibromobenzene (2.0 g, 8.48 mmol) was added, and the suspension was heated at 90 °C for 2 days under argon. The crude was then quenched with H_2O (50 mL) and diluted with EtOAc (100 mL). The organic phase was washed with H_2O (100 mL × 3) and brine (100 mL), dried on Na_2SO_4, and evaporated to a dark solid, purified by a silica plug (Cy/EtOAc 50%) to obtain molecule **12** as a yellow pasty solid (2.8 g, quant.). M.P.: 111−113 °C. ^{1}H-NMR (400 MHz, $CDCl_3$): δ 1.34 (s, 24H), 7.37 (t, 1H, J = 7.8 Hz), 7.90 (dd, 2H, J = 7.4 Hz, J_2 = 1.4 Hz), 8.28 (s, 1H). ^{13}C{^{1}H}-NMR (100 MHz, $CDCl_3$): 25.0, 83.9, 127.2, 137.8, 141.4 (signal for a carbon atom attached to a boron atom absent due to quadrupolar relaxation).^{11}B-{^{1}H}-NMR (128 MHz, $CDCl_3$): δ 29.5 (br). IR: 495, 519, 553, 578, 645, 653, 674, 685, 707, 807, 830, 845, 876, 951, 964, 983, 1009, 1079, 1110, 1138, 1214, 1270, 1305, 1328, 1370, 1456, 1474, 1602, 1669, 2934, 2978, 3436 cm^{-1}. HRMS (ESI-TOF) m/z: $[M + H]^+$ calcd for $C_{18}H_{29}B_2O_4^+$, 331.2253; found, 331.2252. Characterization in accordance with data reported in the literature.[39]

*5,5″-Diphenethyl-[1,1′:3′,1″-terphenyl]-2,2″-diamine (**13**).* 2-Bromo-4-phenethylaniline **6** (1.89 g, 6.87 mmol), diboronic ester **12** (754 mg, 2.28 mmol), $Pd(OAc)_2$ (26 mg, 0.11 mmol), SPhos (94 mg, 0.23 mmol), and KOAc (968 mg, 9.86 mmol) were dissolved in a 5:1 mixture of 1,4-dioxane (30 mL) and H_2O (6 mL). The solution was degassed by five freeze-pump-thaw cycles and stirred at 80 °C for 48 h under argon. The reaction mixture was allowed to cool down to rt, diluted with EtOAc (50 mL), washed with H_2O (50 mL × 3) and brine (100 mL). The organic layer was dried, and the solvent was evaporated under reduced pressure. The black residue was purified by SCC (Cy/EtOAc, 0 to 15%) to yield compound **13** as a light yellow powder (770 mg, 71%). M.P.: 120−122 °C. ^{1}H-NMR (400 MHz, CD_2Cl_2): δ 2.80−2.91 (m, 8H), 3.76 (br s, 4H), 6.70 (d, 2H, J = 7.6 Hz), 6.97−6.99 (m, 4H), 7.13−7.27 (m, 10H), 7.40−7.52 (m, 4H). ^{13}C{^{1}H}-NMR (100 MHz, CD_2Cl_2): δ 37.6, 38.8, 116.2, 126.3, 127.6, 128.1, 128.8, 129.0, 129.1, 129.6, 130.2, 131.0, 132.4, 140.9, 142.2, 142.7. IR: 477, 499, 573, 617, 632, 695, 711, 741, 758, 817, 839, 895, 896, 908, 1029, 1089, 1154, 1251, 1269, 1299, 1307, 1386, 1451, 1469, 1504, 1601, 1617, 2854, 2920, 3025, 3354, 3440 cm^{-1}. HRMS (EI-TOF) m/z: $[M]^+$ calcd for $C_{34}H_{32}N_2^+$, 468.2560; found, 468.2567.

*5,12-Diphenethyl-8H,9H-8,9-diaza-8a-borabenzo[fg]tetracene (**1**).* A solution of BCl_3 (1.0 M in heptane, 250 μL, 0.25 mmol) was added to a solution of terphenyldiamine **13** (100 mg, 0.21 mmol) in anhydrous ODCB (6 mL). The reaction mixture was stirred for 15 min at rt under N_2 before adding $AlCl_3$ (3 mg, 0.023 mmol) and then heated at 150 °C under microwave irradiation for 16 h. The solution was allowed to cool down to rt, and the solvent was removed from the deep brown solution under reduced pressure. The residue was purified by SCC (Cy/EtOAc, 0 to 10%) to yield molecule **1** as a white powder (50 mg, 49%). M.P.: 194−196 °C. ^{1}H-NMR (400 MHz, DMSO-d_6, 50 °C): δ 2.96 (m, 8H), 7.14−7.29 (m, 14H) 7.76 (t, 1H, J = 7.9 Hz), 8.00 (s, 2H), 8.09 (s, 2H), 8.17 (d, 2H, J = 7.9 Hz). ^{13}C{^{1}H}-NMR (100 MHz, DMSO-d_6): δ 37.4, 38.2, 118.8, 119.1, 121.5, 124.3, 126.3, 128.8, 129.0, 129.2, 131.2, 132.5, 139.3, 140.1, 142.5 (signal for a carbon atom attached to a boron atom absent due to quadrupolar relaxation).^{11}B{^{1}H}-NMR (128 MHz, DMSO-d_6): δ 26.5. IR: 531, 580, 628, 649, 670, 699, 750, 750, 798, 849, 875, 916, 1029, 1075, 1288, 1319, 1340, 1420, 1444, 1453, 1468, 1497, 1560, 1603, 2918, 3292 cm^{-1}. HRMS (EI-TOF) m/z: $[M]^+$ calcd for $C_{34}H_{29}BN_2^+$, 476.2418; found, 476.2413.

*5-Mesitylpyridin-2-amine (**10**).* 2-Amino-5-bromopyridine (1.0 g, 5.8 mmol), 2,4,6-trimethylphenylboronic acid (1.1 g, 6.7 mmol), $Pd(OAc)_2$ (70 mg, 0.31 mmol), XPhos (429 mg, 0.90 mmol), and K_3PO_4 (3.7 g, 17.4 mmol) were dissolved in a 5:1 mixture of 1,4-dioxane (10 mL) and H_2O (2 mL). The solution was degassed by three freeze-pump-thaw cycles and stirred at 90 °C for 48 h under nitrogen. The reaction mixture was allowed to cool down to rt, diluted

with EtOAc (50 mL), washed with H_2O (50 mL × 3) and brine (100 mL). The organic layer was dried over $MgSO_4$, and the solvent was evaporated under reduced pressure. The black residue was purified by SCC (Pet. Et/EtOAc, 0 to 30%) to yield compound **10** as an orange powder (1.17 g, 95%). M.P.: 92–94 °C; ^{1}H-NMR (300 MHz, $CDCl_3$): δ 2.04 (s, 6H), 2.32 (s, 3H), 4.50 (bs, 2H), 6.59 (d, 1H, J = 8.7 Hz), 6.94 (s, 2H), 7.25 (dd, 1H, J_1 = 8.7 Hz, J_2 = 1.2 Hz), 7.87 (d, 1H, J = 1.2 Hz). ^{13}C{^{1}H}-NMR (75 MHz, $CDCl_3$): δ 21.0, 21.1, 108.5, 126.8, 128.3, 135.5, 137.0, 137.1, 139.2, 148.2, 157.1. IR: 407, 421, 571, 754, 835, 847, 912, 1011, 1057, 1146, 1234, 1315, 1387, 1439, 1468, 1624, 2913, 3140, 3285, 3464. HRMS (EI-TOF) m/z: $[M]^+$ calcd for $C_{14}H_{16}N_2^+$, 212.1308; found, 212.1313.

*3-Bromo-5-mesitylpyridin-2-amine (**11**).* 5-Mesitylpyridin-2-amine **10** (260 mg, 1.22 mmol) was stirred in CH_3CN (20 mL) with NBS (220 mg, 1.23 mmol) for 12 h. The solution was diluted in CH_2Cl_2 (30 mL); washed with $Na_2S_2O_3$ (sat.) (50 mL), H_2O (50 mL × 3), and brine (50 mL); dried over $MgSO_4$; and evaporated. The resulting residue was purified by SCC (Pet. Et/EtOAc, 0 to 30%) to afford molecule **11** as a pale yellow solid (310 mg, 87%). M.P.: 138–140 °C; ^{1}H-NMR (300 MHz, $CDCl_3$): δ 2.05 (s, 6H), 2.32 (s, 3H), 5.02 (br s, 2H), 6.94 (s, 2H), 7.50 (d, 1H, J = 1.2 Hz), 7.83 (d, 1H, J = 1.2 Hz). ^{13}C{^{1}H}-NMR (75 MHz, $CDCl_3$): δ 21.0, 21.2, 104.4, 128.2, 128.6, 134.2, 137.1, 137.6, 141.5, 147.5, 154.2. IR: 413, 422, 434, 498, 534, 579, 625, 710, 745, 754, 853, 881, 912, 939, 951, 1011, 1057, 1234, 1267, 1288, 1389, 1441, 1468, 1489, 1533, 1593, 1632, 2853, 2916, 3136, 3285, 3470. HRMS (EI-TOF) m/z: $[M + H]^+$ calcd for $C_{14}H_{16}BrN_2^+$, 291.0491; found, 291.0499.

*3,3′-(1,3-Phenylene)bis(5-mesitylpyridin-2-amine) (**15**).* 3-Bromo-5-mesitylpyridin-2-amine **11** (200 mg, 0.69 mmol), diboronic ester **12** (113 mg, 0.34 mmol), $Pd(OAc)_2$ (4 mg, 0.02 mmol), XPhos (32 mg, 0.07 mmol), and K_3PO_4 (437 mg, 2.06 mmol) were dissolved in a 5:1 mixture of 1,4-dioxane (5 mL) and H_2O (1 mL). The solution was degassed by five freeze-pump-thaw cycles and stirred at 90 °C for 20 h under argon. The reaction mixture was allowed to cool down to rt, diluted with CH_2Cl_2 (50 mL), washed with H_2O (40 mL × 3) and brine (50 mL). The organic layer was dried over $MgSO_4$, and the solvent was evaporated under reduced pressure. The black residue was purified by SCC (Pet. Et./EtOAc, 30 to 90%) (5% Et_3N was added to the final eluent to recover the product from the column) to yield compound **15** as a light brown solid (230 mg, 67%). M.P.: 248–250 °C; ^{1}H-NMR (300 MHz, $CDCl_3$): δ 2.09 (s, 12H), 2.32 (s, 6H), 4.65 (br s, 4H), 6.95 (s, 4H), 7.25 (d, 2H, J = 2.1 Hz), 7.53–7.61 (m, 4H), 7.90 (d, 2H, J = 2.1 Hz). ^{13}C{^{1}H}-NMR (75 MHz, $CDCl_3$): δ 21.2, 121.2, 127.6, 128.2, 128.4, 129.2, 130.0, 135.1, 137.0, 137.2, 139.2, 139.4, 147.6, 154.4 (one signal not visible due to overlapping). IR: 411, 426, 494, 538, 573, 635, 714, 793, 849, 912, 1005, 1229, 1391, 1454, 1491, 1558, 1622, 2918, 3140, 3283, 3493. HRMS (EI-TOF) m/z: $[M]^+$ calcd for $C_{34}H_{34}N_4^+$, 498.2778; found, 498.2783.

*5,12-Dimesityl-8H,9H-7,8,9,10-tetraaza-8a-borabenzo[fg]tetracene (**3**).* A solution of BCl_3 (1.0 M in heptane, 210 μL, 0.21 mmol) was added to a solution of terphenyldiamine **15** (100 mg, 0.20 mmol) in anhydrous ODCB (6 mL). The reaction mixture was stirred for 15 min at rt under N_2 before adding $AlCl_3$ (3 mg, 0.023 mmol) and heating at 150 °C under microwave irradiation for 16 h. The solution was allowed to cool down to rt, and the solvent was removed from the deep brown solution under reduced pressure. The residue was purified by SCC (Pet. Et./EtOAc, 30 to 60%) (addition of 5% MeOH to the last eluent was required to remove all products from the column) to yield molecule **3** as a white powder (17 mg, 17%). M.P.: 196–198 °C; ^{1}H-NMR (300 MHz, $CDCl_3$): δ 2.11 (s, 12H, CH_c), 2.37 (s, 6H, CH_e), 7.02 (s, 4H, CH_d), 7.44 (bs, 2H, NH_f), 7.79 (t, 1H, J = 7.9 Hz, CH_h), 8.11 (d, 2H, J = 7.9 Hz, CH_g), 8.15 (d, 2H, J = 2.0 Hz, CH_a), 8.31 (d, 2H, J = 2.0 Hz, CH_b). ^{13}C{^{1}H}-NMR (126 MHz, $CDCl_3$): δ 21.2, 117.4, 120.3, 128.5, 129.5, 131.5, 133.5, 135.4, 137.1, 137.6, 138.4, 148.3, 150.9 (signal for a carbon atom attached to a boron atom absent due to quadrupolar relaxation; one signal for CH_c/CH_e not visible due to overlapping). ^{11}B{^{1}H}-NMR (160 MHz, $CDCl_3$): δ 27.7. IR: 581, 822, 851, 910, 1233, 1281, 1387, 1447, 1576, 1611, 2853, 2920, 2955, 3059, 3221, 3364. HRMS (ESI-TOF) m/z: $[M + H]^+$ calcd for $C_{34}H_{32}BN_4^+$, 507.2709; found, 507.2710.

*2,4,6-Trimethyl-4′-nitro-1,1′-biphenyl (**7**).* 4-Bromonitrobenzene (500 mg, 2.49 mmol), 2,4,6-trimethylphenylboronic acid (447 mg, 2.72 mmol), $[Pd(PPh_3)_4]$ (287 mg, 0.25 mmol), and K_2CO_3 (1.03 g, 7.46 mmol) were dissolved in a 5:1 mixture of 1,4-dioxane (10 mL) and H_2O (2 mL). The solution was degassed by three freeze-pump-thaw cycles and stirred at 90 °C for 48 h under nitrogen. The reaction mixture was allowed to cool down to rt, diluted with CH_2Cl_2 (50 mL), and washed with H_2O (100 mL × 3) and brine (100 mL). The organic layer was dried over $MgSO_4$, and the solvent was evaporated under reduced pressure. The residue was purified by SCC (Pet. Et/CH_2Cl_2, 0 to 20%) to yield compound **7** as a yellow powder (350 mg, 58%). ^{1}H-NMR (300 MHz, $CDCl_3$): δ 2.01 (s, 6H), 2.36 (s, 3H), 6.99 (s, 2H), 7.35 (d, 2H, J = 8.8 Hz), 8.31 (d, 2H, J = 8.8 Hz).^{13}C{^{1}H}-NMR (75 MHz, $CDCl_3$): δ 20.7, 21.1, 123.9, 128.5, 130.6, 135.4, 136.9, 137.8, 147.0, 148.7. IR: 409, 440, 471, 511, 525, 571, 579, 594, 700, 731, 739, 760, 827, 851, 959, 1005, 1028, 1067, 1098, 1105, 1177, 1283, 1312, 1344, 1385, 1396, 1472, 1514, 1599, 1927, 2849, 2947, 3013, 3104. HRMS (EI-TOF) m/z: $[M]^+$ calcd for $C_{15}H_{15}NO_2^+$, 241.1097; found, 241.1108.

*2,4,6-Trimethyl-4′-amino-1,1′-biphenyl (**8**).* Compound **7** (350 mg, 1.45 mmol) was suspended in an EtOH (15 mL) and AcOH (3 mL) solution and stirred for 2 h at rt in the presence of Zn (948 mg, 14.5 mmol). The suspension was filtered through celite to remove the excess of Zn while washing with EtOAc (100 mL). The organic layers were washed with K_2CO_3 (sat.) (100 mL × 2) and brine (100 mL), dried over $MgSO_4$, filtered, and evaporated under reduced pressure. The yellowish residue was purified by SCC (Pet. Et/EtOAc, 20 to 60%) to yield compound **8** as a pale yellow powder (270 mg, 88%). ^{1}H-NMR (300 MHz, $CDCl_3$): δ 2.03 (s, 6H), 2.32 (s, 3H), 3.92 (br s, 2H), 6.77 (d, 2H, J = 8.5 Hz), 6.92–6.98 (m, 4H). ^{13}C{^{1}H}-NMR (75 MHz, $CDCl_3$): δ 21.0, 21.1, 115.5, 128.1, 130.3, 131.7, 136.3, 136.7, 139.1, 144.4. IR: 415, 440, 511, 540, 579, 702, 739, 760, 851, 1005, 1098, 1105, 1177, 1283, 1312, 1344, 1385, 1474, 1514, 1599, 2851, 2918, 2949, 3011, 3352, 3431. HRMS (EI-TOF) m/z: $[M + H]^+$ calcd for $C_{15}H_{18}N^+$, 212.1432; found, 212.1435.

*3-Bromo-2′,4′,6′-trimethyl-[1,1′-biphenyl]-4-amine (**9**).* 4-Mesitylaniline **8** (270 mg, 1.28 mmol) was dissolved in $CHCl_3$ (10 mL) and NBS (228 mg, 1.28 mmol) added at 0 °C. The reaction was allowed to reach rt and stirred for 12 h. The solution was diluted in EtOAc (100 mL), washed with $Na_2S_2O_3$ (sat.) (50 mL), H_2O (100 mL × 3), and brine (100 mL), dried over $MgSO_4$, and evaporated. The orange residue was purified by SCC (Pet. Et/EtOAc, 0 to 5%) to afford molecule **9** as a viscous transparent oil (277 mg, 75%). ^{1}H-NMR (300 MHz, $CDCl_3$): δ 2.02 (s, 6H), 2.31 (s, 3H), 4.57 (br s, 2H), 6.88–6.89 (m, 2H), 6.92 (s, 2H), 7.21 (d, J = 1.8 Hz, 1H). ^{13}C{^{1}H}-NMR (75 MHz, $CDCl_3$): δ 20.9, 21.1, 109.4, 115.8, 128.1, 129.5, 132.5, 133.1, 136.5, 136.7, 137.7, 142.5. IR: 407, 434, 527, 577, 615, 658, 696, 731, 818, 851, 883, 908, 1015, 1040, 1153, 1240, 1267, 1288, 1302, 1375, 1395, 1474, 1508, 1616, 2855, 2916, 3011, 3375, 3472. HRMS (EI-TOF) m/z: $[M + H]^+$ calcd for $C_{15}H_{17}BrN^+$, 290.0539; found, 290.0544.

*2,2′′′′,4,4′′′′,6,6′′′′-Hexamethyl-[1,1′:3′,1″:3″,1‴:3‴,1′′′′-quinquephenyl]-4′,6‴-diamine (**14**).* 3-Bromo-2′,4′,6′-trimethyl-[1,1′-biphenyl]-4-amine **9** (500 mg, 1.72 mmol), diboronic ester **12** (260 mg, 0.78 mmol), $Pd(OAc)_2$ (13 mg, 0.06 mmol), XPhos (47 mg, 0.10 mmol), and K_3PO_4 (470 mg, 2.21 mmol) were dissolved in a 5:1 mixture of 1,4-dioxane (15 mL) and H_2O (3 mL). The solution was degassed by five freeze-pump-thaw cycles and stirred at 80 °C for 48 h under argon. The reaction mixture was allowed to cool down to rt, diluted with EtOAc (50 mL), and washed with H_2O (50 mL × 3) and brine (100 mL). The organic layer was dried over $MgSO_4$, and the solvent was evaporated under reduced pressure. The black residue was purified by SCC (Pet. Et./EtOAc, 30 to 90%) to yield compound **14** as a white-yellow powder (500 mg, 58%). M.P.: 112–114 °C; ^{1}H-NMR (300 MHz, $CDCl_3$): δ 2.09 (s, 12H), 2.32 (s, 6H), 3.86 (br s, 4H), 6.83 (d, 2H, J = 7.4 Hz), 6.92–6.97 (m, 8H), 7.48–7.53 (m, 3H), 7.61 (s, 1H). ^{13}C{^{1}H}-NMR (75 MHz, $CDCl_3$): δ 21.1, 21.1, 116.0, 127.5, 127.9, 128.2, 129.3, 129.7, 129.9, 131.4, 131.6, 136.3,

136.7, 139.0, 140.4, 142.0. IR: 573, 633, 729, 822, 907, 1013, 1030, 1152, 1287, 1375, 1472, 1508, 1616, 2857, 2916, 2947, 3015, 3368, 3460. HRMS (EI-TOF) m/z: $[M + H]^+$ calcd for $C_{36}H_{36}N_2^+$, 497.2951; found, 497.2950.

*5,12-Dimesityl-8H,9H-8,9-diaza-8a-borabenzo[fg]tetracene (**2**).* A solution of BCl_3 (1.0 M in heptane, 210 μL, 0.21 mmol) was added to a solution of terphenyldiamine **14** (100 mg, 0.20 mmol) in anhydrous ODCB (6 mL). The reaction mixture was stirred for 15 min at rt under N_2 before adding $AlCl_3$ (3 mg, 0.023 mmol) and heating at 150 °C under microwave irradiation for 16 h. The solution was allowed to cool down to rt, and the solvent was removed from the deep brown solution under reduced pressure. The residue was purified by SCC (Pet. Et./EtOAc, 30 to 60%) to yield molecule **2** as a white powder (50 mg, 50%). M.P.: 156−158 °C; ^{1}H-NMR (300 MHz, $CDCl_3$): δ 2.12 (s, 12H, CH_c), 2.38 (s, 6H, CH_e), 6.33 (bs, 2H, NH_f), 7.01 (s, 4H, CH_d), 7.08−7.13 (m, 4H, CH_{ai}), 7.74 (t, 1H, J = 8.0 Hz, CH_h), 8.04 (s, 2H, CH_b), 8.10 (d, 2H, J = 7.9 Hz, CH_g). ^{13}C{^{1}H}-NMR (126 MHz, $CDCl_3$): δ 21.15, 21.21, 118.4, 119.2, 122.5, 125.3, 128.3, 129.6, 131.2, 132.7, 136.7, 136.8, 139.2, 139.2, 139.3 (signal for a carbon atom attached to a boron atom absent due to quadrupolar relaxation) ^{11}B{^{1}H}-NMR (160 MHz, $CDCl_3$): δ 27.0. IR: 405, 490, 581, 619, 638, 673, 750, 822, 851, 889, 1028, 1076, 1138, 1188, 1221, 1256, 1283, 1298, 1321, 1375, 1406, 1447, 1460, 1572, 2853, 2916, 2953, 3007, 3385. HRMS (AP-TOF) m/z: $[M + H]^+$ calcd for $C_{36}H_{34}{}^{10}BN_2^+$, 504.2851; found, 504.2833.

■ ASSOCIATED CONTENT

Supporting Information

The Supporting Information is available free of charge at https://pubs.acs.org/doi/10.1021/acs.joc.9b03202.

Synthetic protocols and spectroscopic data for all molecules, computational studies, electrochemical characterization, and titration experiments (PDF)

■ AUTHOR INFORMATION

Corresponding Author

Davide Bonifazi − *Department of Chemistry, University of Namur (UNamur), Namur B-5000, Belgium; School of Chemistry, Cardiff University, Cardiff CF10 3AT, U.K.;* orcid.org/0000-0001-5717-0121; Email: bonifazid@cardiff.ac.uk

Authors

Jonathan Tasseroul − *Department of Chemistry, University of Namur (UNamur), Namur B-5000, Belgium*

Maria Mercedes Lorenzo-Garcia − *School of Chemistry, Cardiff University, Cardiff CF10 3AT, U.K.; Department of Chemical and Pharmaceutical Science, University of Trieste, Trieste 34127, Italy*

Jacopo Dosso − *School of Chemistry, Cardiff University, Cardiff CF10 3AT, U.K.*

François Simon − *Department of Chemistry, University of Namur (UNamur), Namur B-5000, Belgium*

Simone Velari − *Department of Engineering and Architecture, University of Trieste, Trieste 34127, Italy*

Alessandro De Vita − *Department of Engineering and Architecture, University of Trieste, Trieste 34127, Italy; Department of Physics, King's College London, Strand, London WC2R 2LS, U.K.*

Paolo Tecilla − *Department of Chemical and Pharmaceutical Science, University of Trieste, Trieste 34127, Italy*

Author Contributions

[+]These authors equally contributed to this work.

Notes

The authors declare no competing financial interest.

■ ACKNOWLEDGMENTS

The authors gratefully acknowledge the EU through the ERC Starting Grant "COLORLANDS" and the FRS-FNRS. J.T. thanks the FRIA (FNRS) for his doctoral fellowship. D.B. is grateful to the RW through the FLYCOAT project and to Cardiff University for the generous funding. D.B. and P.T. thank the EU for the MC-RISE INFUSION research project. We thank T. Battisti at Cardiff University for the ESP calculations.

■ REFERENCES

(1) Narita, A.; Wang, X.-Y.; Feng, X.; Müllen, K. New advances in nanographene chemistry. *Chem. Soc. Rev.* **2015**, *44*, 6616−6643.

(2) Helten, H. B=N Units as Part of Extended π-Conjugated Oligomers and Polymers. *Chem. − Eur. J.* **2016**, *22*, 12972−12982.

(3) Lorenzo-García, M. M.; Bonifazi, D. Renaissance of an Old Topic: From Borazines to BN-doped Nanographenes. *Chimia. Int. J. Chem.* **2017**, *71*, 550−557.

(4) Giustra, Z. X.; Liu, S.-Y. The State of the Art in Azaborine Chemistry: New Synthetic Methods and Applications. *J. Am. Chem. Soc.* **2018**, *140*, 1184−1194.

(5) Wang, X.-Y.; Wang, J.-Y.; Pei, J. BN heterosuperbenzenes: Synthesis and properties. *Chem. − Eur. J.* **2015**, *21*, 3528−3539.

(6) Liu, Z.; Marder, T. B. B-N versus C-C: How similar are they? *Angew. Chem., Int. Ed.* **2008**, *47*, 242−244.

(7) Helten, H. Doping the Backbone of π-Conjugated Polymers with Tricoordinate Boron: Synthetic Strategies and Emerging Applications. *Chem. - Asian J.* **2019**, *14*, 919−935.

(8) Kervyn, S.; Fenwick, O.; di Stasio, F.; Shin, Y. S.; Wouters, J.; Accorsi, G.; Osella, S.; Beljonne, D.; Cacialli, F.; Bonifazi, D. Polymorphism, fluorescence, and optoelectronic properties of a borazine derivative. *Chem. − Eur. J.* **2013**, *19*, 7771−7779.

(9) Bonifazi, D.; Fasano, F.; Lorenzo-Garcia, M. M.; Marinelli, D.; Oubaha, H.; Tasseroul, J. Boron−nitrogen doped carbon scaffolding: organic chemistry, self-assembly and materials applications of borazine and its derivatives. *Chem. Commun.* **2015**, *51*, 15222−15236.

(10) Dewar, M. J. S.; Marr, P. A. A Derivative of Borazarene. *J. Am. Chem. Soc.* **1962**, *84*, 3782−3782.

(11) Campbell, P. G.; Marwitz, A. J. V.; Liu, S.-Y. Recent Advances in Azaborine Chemistry. *Angew. Chem., Int. Ed.* **2012**, *51*, 6074−6092.

(12) Bosdet, M. J. D.; Piers, W. E.; Sorensen, T. S.; Parvez, M. 10a-Aza-10b-borapyrenes: Heterocyclic Analogues of Pyrene with Internalized BN Moieties. *Angew. Chem., Int. Ed.* **2007**, *46*, 4940−4943.

(13) Chissick, S. S.; Dewar, M. J. S.; Maitlis, P. M. New heteraromatic compounds containing two boron atoms. *Tetrahedron Lett.* **1960**, *1*, 8−10.

(14) Bosdet, M. J. D.; Jaska, C. A.; Piers, W. E.; Sorensen, T. S.; Parvez, M. Blue Fluorescent 4a-Aza-4b-boraphenanthrenes. *Org. Lett.* **2007**, *9*, 1395−1398.

(15) Dewar, M. J. S.; Dietz, R. 546. New heteroaromatic compounds. Part III. 2,1-Borazaro-naphthalene (1,2-dihydro-1-aza-2-boranaphthalene). *J. Chem. Soc.* **1959**, 2728−2730.

(16) Wisniewski, S. R.; Guenther, C. L.; Argintaru, O. A.; Molander, G. A. A Convergent, Modular Approach to Functionalized 2,1-Borazaronaphthalenes from 2-Aminostyrenes and Potassium Organotrifluoroborates. *J. Org. Chem.* **2014**, *79*, 365−378.

(17) Ishibashi, J. S. A.; Marshall, J. L.; Mazière, A.; Lovinger, G. J.; Li, B.; Zakharov, L. N.; Dargelos, A.; Graciaa, A.; Chrostowska, A.; Liu, S.-Y. Two BN Isosteres of Anthracene: Synthesis and Characterization. *J. Am. Chem. Soc.* **2014**, *136*, 15414−15421.

(18) van de Wouw, H. L.; Lee, J. Y.; Siegler, M. A.; Klausen, R. S. Innocent BN bond substitution in anthracene derivatives. *Org. Biomol. Chem.* **2016**, *14*, 3256−3263.
(19) Fingerle, M.; Stocker, S.; Bettinger, H. F. New Synthesis of a Dibenzoperylene Motif Featuring a Doubly Boron−Nitrogen-Doped Bay Region. *Synthesis* **2019**, *51*, 4147−4152.
(20) Hatakeyama, T.; Hashimoto, S.; Seki, S.; Nakamura, M. Synthesis of BN-Fused Polycyclic Aromatics via Tandem Intramolecular Electrophilic Arene Borylation. *J. Am. Chem. Soc.* **2011**, *133*, 18614−18617.
(21) Stępień, M.; Gońka, E.; Żyła, M.; Sprutta, N. Heterocyclic Nanographenes and Other Polycyclic Heteroaromatic Compounds: Synthetic Routes, Properties, and Applications. *Chem. Rev.* **2017**, *117*, 3479−3716.
(22) For OLED applications, see: (a) Hatakeyama, T.; Shiren, K.; Nakajima, K.; Nomura, S.; Nakatsuka, S.; Kinoshita, K.; Ni, J.; Ono, Y.; Ikuta, T. Ultrapure Blue Thermally Activated Delayed Fluorescence Molecules: Efficient HOMO-LUMO Separation by the Multiple Resonance Effect. *Adv. Mater.* **2016**, *28*, 2777−2781. (b) Fresta, E.; Dosso, J.; Cabanillas-González, J.; Bonifazi, D.; Costa, R. D. Origin of the Exclusive Ternary Electroluminescent Behavior of BN-Doped Nanographenes in Efficient Single-Component White Light-Emitting Electrochemical Cells. *Adv. Funct. Mater.* **2020**, 1906830.
(23) Georgiou, I.; Kervyn, S.; Rossignon, A.; De Leo, F.; Wouters, J.; Bruylants, G.; Bonifazi, D. Versatile Self-Adapting Boronic Acids for H-Bond Recognition: From Discrete to Polymeric Supramolecules. *J. Am. Chem. Soc.* **2017**, *139*, 2710−2727.
(24) Lee, H.; Fischer, M.; Shoichet, B. K.; Liu, S.-Y. Hydrogen Bonding of 1,2-Azaborines in the Binding Cavity of T4 Lysozyme Mutants: Structures and Thermodynamics. *J. Am. Chem. Soc.* **2016**, *138*, 12021−12024.
(25) Liu, Y.; Liu, S.-Y. Exploring the strength of a hydrogen bond as a function of steric environment using 1,2-azaborine ligands and engineered T4 lysozyme receptors. *Org. Biomol. Chem.* **2019**, *17*, 7002−7006.
(26) Dosso, J.; Tasseroul, J.; Fasano, F.; Marinelli, D.; Biot, N.; Fermi, A.; Bonifazi, D. Synthesis and Optoelectronic Properties of Hexa-peri-hexabenzoborazinocoronene. *Angew. Chem., Int. Ed.* **2017**, *56*, 4483−4487.
(27) Numano, M.; Nagami, N.; Nakatsuka, S.; Katayama, T.; Nakajima, K.; Tatsumi, S.; Yasuda, N.; Hatakeyama, T. Synthesis of Boronate-Based Benzo[fg]tetracene and Benzo[hi]hexacene via Demethylative Direct Borylation. *Chem. - Eur. J.* **2016**, *22*, 11574−11577.
(28) Wang, X.; Zhang, F.; Schellhammer, K. S.; Machata, P.; Ortmann, F.; Cuniberti, G.; Fu, Y.; Hunger, J.; Tang, R.; Popov, A. A.; Berger, R.; Müllen, K.; Feng, X. Synthesis of NBN-Type Zigzag-Edged Polycyclic Aromatic Hydrocarbons: 1,9-Diaza-9a-boraphenalene as a Structural Motif. *J. Am. Chem. Soc.* **2016**, *138*, 11606−11615.
(29) White, N. G. Recent advances in self-assembled amidinium and guanidinium frameworks. *Dalton Trans.* **2019**, *48*, 7062−7068.
(30) Adjabeng, G.; Brenstrum, T.; Frampton, C. S.; Robertson, A. J.; Hillhouse, J.; McNulty, J.; Capretta, A. Palladium complexes of 1,3,5,7-tetramethyl-2,4,8-trioxa-6-phenyl-6- phosphaadamantane: Synthesis, crystal structure and use in the Suzuki and Sonogashira reactions and the α-arylation of ketones. *J. Org. Chem.* **2004**, *69*, 5082−5086.
(31) Biswas, S.; Müller, M.; Tönshoff, C.; Eichele, K.; Maichle-Mössmer, C.; Ruff, A.; Speiser, B.; Bettinger, H. F. The overcrowded borazine derivative of hexabenzotriphenylene obtained through dehydrohalogenation. *Eur. J. Org. Chem.* **2012**, *2012*, 4634−4639.
(32) Müller, M.; Behnle, S.; Maichle-Mössmer, C.; Bettinger, H. F. Boron−nitrogen substituted perylene obtained through photocyclisation. *Chem. Commun.* **2014**, *50*, 7821.
(33) Boiocchi, M.; Del Boca, L.; Gómez, D. E.; Fabbrizzi, L.; Licchelli, M.; Monzani, E. Nature of Urea−Fluoride Interaction: Incipient and Definitive Proton Transfer. *J. Am. Chem. Soc.* **2004**, *126*, 16507−16514.
(34) Esteban-Gómez, D.; Fabbrizzi, L.; Licchelli, M. Why, on Interaction of Urea-Based Receptors with Fluoride, Beautiful Colors Develop. *J. Org. Chem.* **2005**, *70*, 5717−5720.
(35) Goursaud, M.; De Bernardin, P.; Dalla Cort, A.; Bartik, K.; Bruylants, G. Monitoring fluoride binding in DMSO: Why is a singular binding behavior observed? *Eur. J. Org. Chem.* **2012**, *2012*, 3570−3574.
(36) Liang, F.; Lindsay, S.; Zhang, P. 1,8-Naphthyridine-2,7-diamine: A potential universal reader of Watson-Crick base pairs for DNA sequencing by electron tunneling. *Org. Biomol. Chem.* **2012**, *10*, 8654−8659.
(37) Hunter, C. A. Quantifying intermolecular interactions: Guidelines for the molecular recognition toolbox. *Angew. Chem., Int. Ed.* **2004**, *43*, 5310−5324.
(38) Kuzmič, P. Program DYNAFIT for the analysis of enzyme kinetic data: Application to HIV proteinase. *Anal. Biochem.* **1996**, *237*, 260−273.
(39) Fu, S. H.; Higuchi, M.; Kurth, D. G. Diverse synthesis of novel bisterpyridines via Suzuki-type cross-coupling. *Org. Lett.* **2007**, *9*, 559−562.
(40) Blight, B. A.; Hunter, C. A.; Leigh, D. A.; McNab, H.; Thomson, P. I. T. An AAAA−DDDD quadruple hydrogen-bond array. *Nat. Chem.* **2011**, *3*, 244−248.
(41) (a) Wilson, A. J. Hydrogen Bonding Receptors for Molecular Guests, In *Supramolecular Chemistry: From Molecules to Nanomaterials*; Vol 3, García-España, E.; Gale, P. A.; Steed, J. W., Eds.; Wiley, 2012, 1325−1344; (b) Wilson, A. J. Non-Covalent Polymer Assembly Using Arrays of Hydrogen-Bonds. *Soft Matter* **2007**, *3*, 409−425.
(42) Eaton, D. F. Reference materials for fluorescence measurement. *J. Photochem. Photobiol. B Biol.* **1988**, *2*, 523−531.
(43) Crosby, G. A.; Demas, J. N. Measurement of photoluminescence quantum yields. Review. *J. Phys. Chem.* **1971**, *75*, 991−1024.
(44) Giannozzi, P.; Baroni, S.; Bonini, N.; Calandra, M.; Car, R.; Cavazzoni, C.; Ceresoli, D.; Chiarotti, G. L.; Cococcioni, M.; Dabo, I.; Dal Corso, A.; de Gironcoli, S.; Fabris, S.; Fratesi, G.; Gebauer, R.; Gerstmann, U.; Gougoussis, C.; Kokalj, A.; Lazzeri, M.; Martin-Samos, L.; Marzari, N.; Mauri, F.; Mazzarello, R.; Paolini, S.; Pasquarello, A.; Paulatto, L.; Sbraccia, C.; Scandolo, S.; Sclauzero, G.; Seitsonen, A. P.; Smogunov, A.; Umari, P.; Wentzcovitch, R. M. QUANTUM ESPRESSO: a modular and open-source software project for quantum simulations of materials. *J. Phys.: Condens. Matter* **2009**, *21*, 395502.
(45) Vanderbilt, D. Soft self-consistent pseudopotentials in a generalized eigenvalue formalism. *Phys. Rev. B* **1990**, *41*, 7892−7895.
(46) Becke, A. D. Density-functional exchange-energy approximation with correct asymptotic behavior. *Phys. Rev. A* **1988**, *38*, 3098−3100.
(47) Lee, C.; Yang, W.; Parr, R. G. Development of the Colle-Salvetti correlation-energy formula into a functional of the electron density. *Phys. Rev. B* **1988**, *37*, 785−789.
(48) Kokalj, A. Computer graphics and graphical user interfaces as tools in simulations of matter at the atomic scale. *Comput. Mater. Sci.* **2003**, *28*, 155−168.